NMR in Biomedicine

WILEY

NMR IN BIOMEDICINE

RESEARCH ARTICLE OPEN ACCESS

The Goldilocks Zone for 3-T MRS Studies Using Semi-LASER: Determining the Optimal Balance Between Repetition Time and Scan Time

Alex G. Ensworth[1,2] | Laura R. Barlow[3,4] | Piotr Kozlowski[1,2,3,4] | Erin L. MacMillan[3,4,5] | Cornelia Laule[1,2,3,4,5,6]

[1]Physics & Astronomy, University of British Columbia, Vancouver, Canada | [2]International Collaboration on Repair Discoveries (ICORD), University of British Columbia, Vancouver, Canada | [3]Radiology, University of British Columbia, Vancouver, Canada | [4]UBC MRI Research Centre, University of British Columbia, Vancouver, Canada | [5]Djavad Mowafaghian Centre for Brain Health, University of British Columbia, Vancouver, Canada | [6]Pathology & Laboratory Medicine, University of British Columbia, Vancouver, Canada

Correspondence: Cornelia Laule (claule@physics.ubc.ca)

Received: 24 September 2024 | **Revised:** 3 May 2025 | **Accepted:** 6 May 2025

Funding: AE receives funding support from an MS Canada Doctoral Studentship Award. PK and CL are recipients of Natural Sciences and Engineering Research Council of Canada (NSERC) Discovery Grants. ELM received salary support from Philips Canada.

Keywords: brain | FSL-MRS | magnetic resonance spectroscopy | metabolites | MRS | semi-LASER | T_1 relaxation

ABSTRACT

^{1}H-MR spectroscopy studies often use a short TR to reduce scan time. However, this causes significant T_1-weighting (T_1w), which can alter metabolite estimates due to acquisition factors rather than biochemistry. Our goal was to determine the optimal balance between scan time and TR that minimizes T_1w effects in semi-LASER MRS at 3 T. Spectra were acquired in the posterior cingulate cortex of five healthy volunteers (2 male/3 female, mean age 25 ± 2 years) and analyzed using FSL-MRS. The SNR and metabolite estimates of five metabolites were compared at TR = 2, 5, and 8 s, under conditions of "similar scan time" with varying acquisition numbers and "constant number of acquisitions" with varying scan times. T_1 relaxation times derived from metabolite estimates were compared to literature. With a 25% longer scan time, $SNR_{TR=5s}$ was 34% higher and $SNR_{TR=2s}$ was 29% higher than $SNR_{TR=8s}$ for data with "similar scan times." Using a TR = 5 s or longer, the SNR per minute is consistent for metabolites with T_1s less than 2 s. Metabolite estimate trends were similar for the two different scenarios of "similar scan time" and "same number of acquisitions," where all metabolite estimates were obtained without metabolite T_1 correction. The largest metabolite estimates were found at TR = 8 s, they were 10–15% lower at TR = 5 s and 15–30% lower at TR = 2 s. T_1 values agreed with literature values. At TR = 2 s, SNR per minute and metabolite estimates were lower due to reduced signal availability via T_1w effects. TR = 8 s had the least amount of T_1w effects, but results in lower SNR per minute. TR = 5 s had enough signal recovery to be robust to T_1w effects, and yielded the largest SNR for similar scan times, with a clinically feasible scan time of 5 m 40 s. Using semi-LASER MRS with a TR = 5 s is recommended to improve the sensitivity of MRS to changes in metabolite estimates.

Abbreviations: ap, anterior–posterior direction; CSF, cerebrospinal fluid; FAST, FMRIB Automatic Segmentation Tool; fh, foot-head direction; FMRIB, functional MRI of the brain; FOV, field of view; FSL, FMRIB Software Library; FWHM, full-width half-maximum; Glu, glutamate; GM, grey matter; HLSVD, Hankel Lanczos singular value decomposition; IR, inversion recovery; mI, myo-inositol; MPRAGE, magnetization prepared rapid gradient echo; NAA, N-acetyl aspartate; NSA, number of spectra acquired; PCC, posterior cingulate cortex; PS, progressive saturation; rl, right–left direction; semi-LASER, semi-adiabatic localization by adiabatic selective refocusing; T_1w, T_1-weighting; tCho, total choline; tCr, total creatine; WM, white matter.

1 | Introduction

Magnetic resonance spectroscopy (MRS) can provide quantitative information about the biochemical makeup, or metabolites, of the brain. However, MRS data quality and the quantification of metabolites can be influenced by a variety of data collection parameters including the localization sequence, the water suppression method, the TE, and the TR [1, 2]. Many clinical MRS studies opt for a short TR of 2 s to reduce scan time. With a shorter TR, it is possible to collect more acquisitions during the MRS experiment, which is assumed to increase the SNR per unit time [3–7]. However, using a TR that is less than approximately five times the length of the metabolite longitudinal relaxation time leads to significant T_1-weighting (T_1w) effects, which means there is not enough time between repeated acquisitions for the signal to completely recover. Consequently, less signal is available to be excited on the following acquisition, which leads to an apparent reduction of the metabolite estimates due to these T_1w effects, without correction for T_1 values. For example, at a magnetic field strength of 3 T, some brain metabolites have T_1 relaxation times of ~1.5 s [8–11]. If MRS data is collected using a TR of 2 s, these metabolites will be heavily T_1w, while other metabolites with shorter T_1 relaxation times will be less affected. Given that T_1 times increase with field strength, and that more neurological studies are being conducted at 3 T, and even 7 T, the potential issue of T_1w in MRS studies needs to be considered [12, 13].

The MRS expert consensus series directly addresses the impact of short TR on metabolite quantification, stating that T_1w effects need to be corrected for using known metabolite T_1 relaxation times, and that a TR <3 s is more practical for human studies [14]. However, the consensus T_1 relaxation times are different for each metabolite, and can change based on brain region, age, and sex of the participant, and/or any pathology or disease present [15, 16].

Estimating metabolite T_1 relaxation times is challenging and time-consuming as multiple MRS acquisitions are required to populate the T_1 relaxation curve. Metabolite T_1 times are typically only calculated for high SNR metabolites, with estimates for low SNR metabolites being impractical. Measuring the T_1 of all metabolites present in all brain regions, all ages, sexes, pathologies, and field strengths quickly makes for a Sisyphean task. Therefore, relying on a correction method to undo the T_1w effects imposed by using a short TR seriously diminishes the accuracy of MRS and hinders cross-study agreement.

Using a longer TR reduces the effects of T_1w, minimizes the variability in T_1 corrections imparted on metabolite estimates, and provides results that more accurately reflect true metabolite estimates. A longer TR will also enable more accurate comparisons across studies and in different diseases or conditions. However, increasing the TR either increases the total scan time or it requires one to reduce the number of acquisitions to maintain the same total scan time, potentially reducing the SNR. The overall goal of our study was to determine the optimal balance between TR and scan time to minimize T_1w effects. Specifically, we characterized the effect of different TRs on SNR and metabolite estimates using semi-LASER MRS at 3 T, under conditions of similar scan time with varying acquisition numbers, and constant number of acquisitions with varying scan times. We also compared metabolite T_1 relaxation times determined using a limited number of TRs to known literature values.

2 | Materials and Methods

2.1 | Data Collection

MRS data was acquired on a 3-T Philips Ingenia Elition X with a ^{1}H 32-channel receive-only head coil at the UBC MRI Research Centre (RRID:SCR_025374). Five healthy volunteers (2M/3F, mean age 25 ± 2 years) were scanned after obtaining written, informed consent, as approved by the local clinical research ethics board. Data collection began with a structural, 3D-T_1 scan (MPRAGE, TE/TR = 4.3/2400 ms, 225 slices, 0.8-mm isotropic resolution, FOV [ap, fh, rl] = 256 mm × 256 mm × 180 mm). MRS signal localization was acquired in a $30 \times 20 \times 13\,mm^3$ (7.8 cm^3) voxel in the posterior cingulate cortex (PCC) via semi-LASER [17] (excitation pulse: maximum $B_1 = 22\,\mu T$, average $B_1 = 3.04\,\mu T$, duration = 4.38 ms, bandwidth = 3710 Hz; adiabatic pulses: maximum $B_1 = 22\,\mu T$, average $B_1 = 18.33\,\mu T$, duration = 4.45 ms, bandwidth = 6597 Hz) in the PCC (TE = 32 ms, spectral bandwidth = 2000 Hz, 2048 samples, manufacturer-provided "Excitation" option, which is a two-pulse variation on chemical shift selective [CHESS] water suppression). The SAR levels of the semi-LASER sequence remained consistent across TRs and well below the scanner-imposed limit, and the consistent B_1 amplitudes across TRs ensured consistent volume localization. Spectra were obtained at three different TRs for each volunteer (TR = 2 s, number of spectra acquired [NSA] = 128; TR = 5 s, NSA = 64; TR = 8 s, NSA = 64). All acquisitions for each TR were acquired in one scan and the order of scans was randomized for each volunteer (V1: TR = 8, 2, 5 s; V2: TR = 5, 8, 2 s; V3: TR = 8, 2, 5 s; V4: 2, 5, 8 s; V5: TR = 2, 8, 5 s). Acquisition numbers were in multiples of 32 to account for the 32-step phase cycling scheme of the semi-LASER localization sequence [17]. Additionally, each scan began with four dummy scans and four unsuppressed-water acquisitions. All transients were coil-combined on the scanner, then saved individually to allow for comparisons between similar scan times at different TRs and between the same NSA at different TRs. The breakdown of how data was separated into these two categories is summarized in Table 1. In situations where acquisitions were removed (TR = 2 s, 64 NSA and TR = 8 s, 32 NSA), the second half of the acquisitions were excluded to simulate an MRS acquisition with the desired NSA. Power optimization calibration and manufacturer-provided B_0 shimming were conducted once, at the start of the first MRS scan.

2.2 | Data Analysis

The 3D-T_1 scan was segmented with the Functional MRI of the Brain (FMRIB) Software Library (FSL), using the FMRIB Automatic Segmentation Tool (FAST) [18] into components of white matter (WM), grey matter (GM), and cerebrospinal fluid (CSF) for absolute quantification. The basis set was simulated in MATLAB using FID-A with real pulse shapes and real voxel dimensions to simulate a basis set for shaped pulses [19]. The

TABLE 1 | A detailed breakdown of data collection. The first section, titled MRS data acquired, outlines the three different experiments collected, the order of which was randomized for each volunteer. The remaining two sections illustrate how, during postprocessing, the acquisitions were modified to produce a set of data that kept the scan time similar, and the number of acquisitions were kept the same, with varying scan time. Scan times marked with an asterisk denote hypothetical approximated scan time derived from calculation. When the number of acquisitions were reduced from the MRS data acquired section, the second half of acquisitions were removed to simulate the equivalent scan with fewer acquisitions. Acquisition number was constrained to a multiple of 32 due to the 32-step phase cycle of semi-LASER.

MR spectroscopy acquisition specifications			
	Repetition time (s)	**Number of acquisitions**	**Scan time**
MRS data acquired	2	128	4 m 24 s
	5	64	5 m 40s
	8	64	9 m 04 s
Similar scan time (~5 min)			
MRS data averaged in postprocessing	2	128	4 m 24 s
	5	64	5 m 40s
	8	32	4 m 48 s*
Same number of acquisitions (64)			
MRS data averaged in postprocessing	2	64	2 m 16 s*
	5	64	5 m 40s
	8	64	9 m 04 s

following metabolites were included in the basis set: alanine (Ala), aspartic acid (Asp), beta-hydroxybutyrate (bHB), creatine (Cr), gamma-aminobutyric acid (GABA), glucose (Glc), glutamine (Gln), glutamate (Glu), glycine (Gly), glycerylphosphorylcholine (GPC), glutathione (GSH), myo-inositol (mI), lactate (Lac), N-acetyl aspartate (NAA), NAA glutamate (NAAG), phosphorylcholine (PCh), phosphocreatine (PCr), phosphorylethanolamine (PE), scyllo-inositol (Scyllo), and taurine (Tau). Synthetic macromolecular basis signals were included and were generated using the built-in functionality of FSL-MRS, with a relative amplitude of 0.5 and a Lorentzian width of 70 Hz. Macromolecular peaks were added at 0.9, 1.2, 1.4, 1.6, 2.1, 3.0, and 3.9 ppm. These locations were chosen based on the macromolecular peaks identified in a previous analysis using LC Model. After fitting the MRS data, metabolite estimates of GPC and PCh were added together to create metabolite estimates for total choline (tCho). Similarly, Cr and PCr estimates were combined to produce total creatine (tCr).

The MRS data were processed and analyzed using FSL-MRS, version 2.1.12 [20]. The FIDs were first zero-padded by 2048 points to a total of 4096 points. Data processing then involved: (1) frequency alignment, (2) bad average removal, (3) frequency alignment, (4) transient combination, (5) eddy-current correction, (6) water peak removal via Hankel Lanczos singular value decomposition (HLSVD) [21], and (7) phase correction. Frequency alignment was conducted between 4.5 and 4.8 ppm to capture the residual water peak as this proved more robust than using NAA. The frequency alignment of each data set was visually inspected for accuracy. Additionally, the constants.py file in the FSL-MRS utilities package was accessed, and the relaxation parameters at 3 T were modified. The "STANDARD_T1" parameter for "METAB" was changed from 1.29 to 0.001, and the "STANDARD_T2" parameter for "METAB" was changed from 0.194 to 100. No "H2O-" parameters were modified. This was done to remove any T_1 and T_2 relaxation correction approximations to metabolite signals imposed by the FSL-MRS fitting software. Relaxation correction effects on water peak areas remained.

The metabolite estimates and the SNR for five commonly reported metabolites (NAA, tCho, tCr, mI, and Glu) were compared across the different TRs for scenarios of similar scan time with varying NSA and same NSA with varying scan time, according to Table 1.

SNR: SNR was measured using the definition suggested by Ernst et al. [22]. It is the ratio of the peak height of the fitted metabolite basis spectrum and the standard deviation of a pure noise region of the spectrum, after a matched filter has been applied to both. The amount of noise in the spectrum relies on the number of points in the FID, so applying a matched filter helps normalize the number of points included. The matched filter is apodization with a width set to the peak width. This simultaneously ensures that SNR is maximized while also allowing SNR to be reported for each metabolite with a different matched filter applied to each metabolite [20]. The standard deviation of the noise is estimated from the original spectrum in a region that is less than −2 ppm or greater than 10 ppm, where no signal is expected. To facilitate comparison between TRs, the SNR values of NAA for each volunteer were normalized to a TR = 8 s. A TR of 8 s was chosen as all metabolite signals with T_1s less than or equal to 1.5 s are considered to be > 99% recovered after 8 s. Normalization to TR = 8 s will result in any variability that may exist at a TR = 8 s being translated into increased variability at TRs of 2 and 5 s.

Due to the phase cycle restrictions imposed by semi-LASER, using a TR = 5 s results in a scan time that is about 1.25 times longer than when using both TR = 2 s and TR = 8 s in the "similar scan time" situation. A more direct comparison of SNR between scenarios was evaluated by calculating the SNR per unit scan time for the "similar scan time" parameters according to Table 1. The measured SNR obtained using FSL-MRS was divided by the product of TR and NSA (i.e., the time in which water-suppressed data were being collected). This is reported as SNR per minute as scan times are typically compared on the order of minutes. The expected SNR per minute was calculated as follows, using TR = 8 s as the reference. As $SNR \propto \sqrt{NSA}$, the first step was to take the measured SNR (TR = 8 s, NSA = 32) and multiply it by the square root of the ratio of additional acquisitions (i.e., TR = 2 s: $\sqrt{128/32}$; TR = 5 s: $\sqrt{64/32}$). This product was then multiplied by the ratio of T_1w effects: $M_z(TR = 2s, 5s) / M_z(TR = 8s)$, where $M_z(TR)$ is the magnetization recovery along the z-axis as a function of TR, given by the saturation recovery equation

$$M_z(TR) = M_0\left[1 - \exp\left(-\frac{TR}{T_1}\right)\right] \quad (1)$$

and M_0 is the initial magnetization. Finally, this was divided by the data acquisition time in minutes, given as $TR \times NSA$ (TR = 2 s: $[2s \times 128 / 60s]$; TR = 5 s: $[5s \times 64 / 60s]$). This whole pipeline can be represented as

$$SNR_{target}/minute = SNR_{TR=8s,NSA=32} \times \sqrt{\frac{NSA_{target}}{32}} \times \frac{M_z(TR_{target})}{M_z(TR=8s)} \times \frac{60\ s}{TR_{target} \times NSA_{target}}, \quad (2)$$

where the subscript of "target" represents the corresponding value for TR = 2 s, or TR = 5 s.

2.3 | Metabolite Estimates

Metabolite estimates were calculated with FSL-MRS using unsuppressed-water acquisitions for water scaling and were corrected with the FSL FAST voxel segmentation values for GM, WM, and CSF. To evaluate the effect of TR on metabolite estimates, for each metabolite, the FSL-MRS-derived metabolite estimates at TR = 2 s and TR = 5 s were normalized to the derived metabolite estimate at TR = 8 s. The normalized metabolite estimate data were then averaged across volunteers at each TR and graphed.

2.4 | Metabolite T_1

Metabolite T_1 relaxation times were calculated by fitting metabolite estimates to the saturation recovery equation (Equation 1), using the maximum NSA for each TR (TR2 × 128, TR5 × 64, and TR8 × 64). For T_1 fitting only, the spectra for each volunteer were refit with FSL-MRS. The only parameter modification was to use the water reference data for the corresponding TR = 8 s data of that volunteer for every TR. A single T_1 value was obtained from this fit for a specific metabolite for each volunteer. Then, T_1 values across all five volunteers were combined to provide a mean and standard deviation for each metabolite, yielding an average value with uncertainty. The resultant T_1 values were compared to existing literature values in similar brain regions.

3 | Results

An example of the voxel location, along with sample spectra are shown in Figure 1.

3.1 | SNR

Figure 2 demonstrates the effect of TR on SNR for NAA, for both scenarios of similar scan time with varying NSA and constant NSA with varying scan time without metabolite T_1 correction. Comparisons of SNR for other metabolites can be found online at https://tr-in-mrs.streamlit.app/. For spectra obtained with a similar scan time and varying NSA, compared to a TR = 8 s, the average SNR was 29% higher for TR = 2 s and 34% higher for TR = 5 s with a 25% longer scan duration. For spectra obtained with a constant NSA and varying scan time, compared to a TR = 8 s, the SNR was 29% lower for TR = 2 s and 2% lower for TR = 5 s. Full-width half-maximum (FWHM) values for NAA were relatively constant across TRs, with 4.43

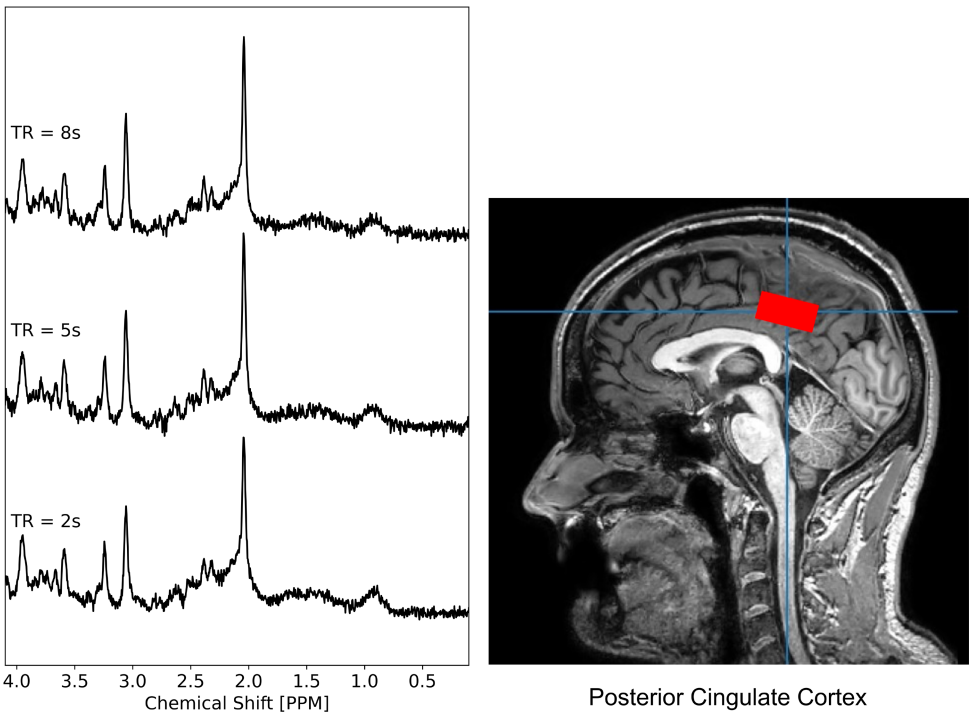

FIGURE 1 | A sample spectrum for each TR (TR = 2 s has 128 NSA, TR = 5 and 8 s have 64 NSA), obtained via semi-LASER MRS in the posterior cingulate cortex of one healthy volunteer. Spectral analysis was done using FSL-MRS. Spectra were normalized to the metabolite estimate of N-acetyl aspartate (NAA) to account for SNR differences due to different acquisition parameters.

A) Similar scan time

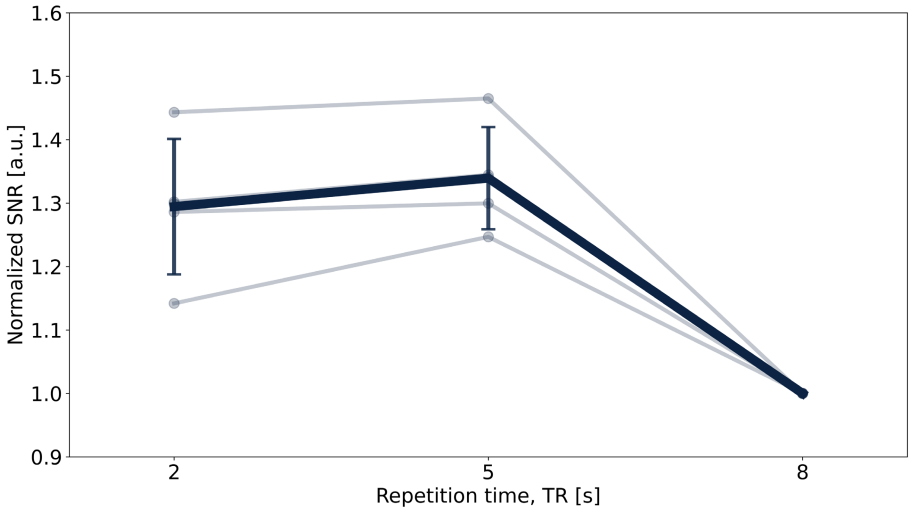

Acq. Time	4m 24s	5m 40s	4m 48s
NSA	128	64	32
SNR	Mean: 55.5 Range: 48.4-59.0	Mean: 57.5 Range: 50.0-61.7	Mean: 43.1 Range: 37.2-49.5
% CRLB	Mean: 1.23% Range: 0.97-2.01%	Mean: 1.83% Range: 1.38-2.36%	Mean: 2.00% Range: 1.56-2.34%

B) Same number of acquisitions (64)

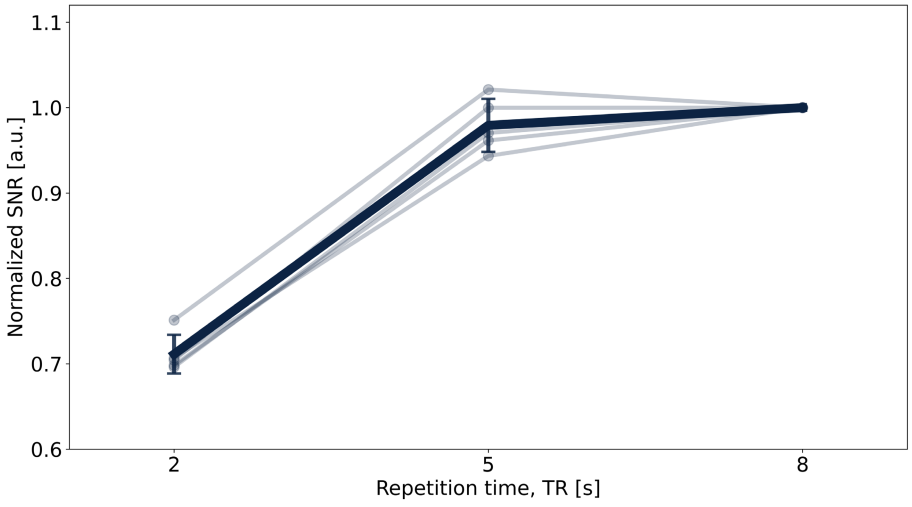

Acq. Time	2m 16s	5m 40s	9m 04s
NSA	64	64	64
SNR	Mean: 41.8 Range: 35.9-46.2	Mean: 57.5 Range: 50.0-61.7	Mean: 58.8 Range: 51.5-65.4
% CRLB	Mean: 1.65% Range: 1.21-2.42%	Mean: 1.83% Range: 1.38-2.36%	Mean: 1.80% Range: 0.89-2.37%

FIGURE 2 | The SNR of N-acetyl aspartate (NAA) is plotted for each volunteer against different repetition times. In panel (A), the SNR resulting from acquisition times of approximately 5 min is shown, while in panel (B), the SNR resulting from 64 transients is shown. For each volunteer, the SNR value was normalized to the associated SNR value at a TR of 8 s. SNR values for all volunteers at each TR were averaged together and are shown in bold. The standard deviation of volunteer data at TR = 2 s and TR = 5 s is represented as error bars. Average and range of absolute SNR and % CRLB are included for each situation below the plot.

at TR = 2 s, 4.34 at TR = 5 s, and 4.35 at TR = 8 s for both similar scan time and same number of acquisitions. The full range of FWHM across all volunteers and TRs is 4.02–4.97. More information can be found online in the application. Figure 3 shows the SNR per minute for NAA at each TR, along with the expected SNR per minute with and without T_1w. The SNR per minute averaged across five healthy volunteers was found to be 10.1 ± 1.1 at TR = 8 s, 10.8 ± 0.8 at TR = 5 s, and 13.0 ± 1.0 at TR = 2 s.

3.2 | Metabolite Estimates

Figure 4 shows the variation of metabolite estimates as a function of TR for the two scenarios of similar scan time with varying NSA, and constant NSA with varying scan time without metabolite T_1 correction. Average metabolite estimates were 15%–30% lower for TR = 2 s compared to TR = 8 s, while they were only 10%–15% lower at TR = 5 s. This trend was observed in both scenarios of similar scan time with varying NSA and same NSA with varying scan time.

3.3 | Metabolite T_1

Metabolite T_1 relaxation times output from the fit of Equation (1) are reported in Table 2 and plotted in Figure 5. T_1 values averaged across volunteers were NAA: 1.53 ± 0.08 s, tCho: 1.16 ± 0.17 s, tCr: 1.36 ± 0.12 s, mI: 1.24 ± 0.12 s, and Glu: 1.38 ± 0.12 s.

4 | Discussion

T_1w can significantly impact the accuracy of MRS in quantifying brain metabolite levels. With the increasing trend of using shorter TRs to reduce scan duration and allow for more acquisitions, our study aimed to find the optimal balance between TR and scan time that minimizes T_1w effects. We demonstrated that using a TR = 5 s, with half the number of acquisitions compared to TR = 2 s, results in spectra with higher SNR in a clinically feasible scan time while being more robust to variations in metabolite T_1 relaxation times.

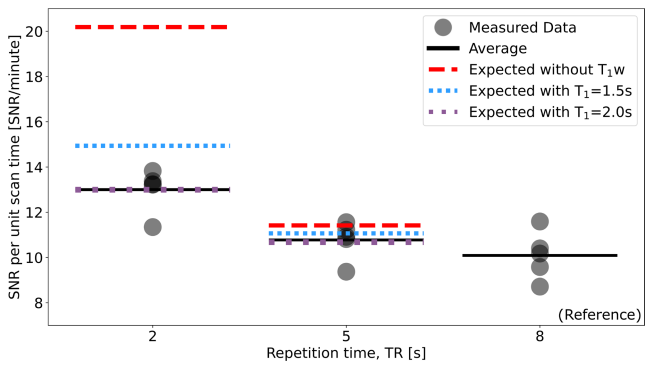

FIGURE 3 | The SNR per unit scan time for NAA is calculated for each volunteer at each TR, represented as dots, by determining the ratio of SNR to scan time (TR*NSA) required for that TR. The SNR corresponding to data for a similar scan time was used in this calculation: TR = 2 s and 128 NSA; TR = 5 s and 64 NSA; and TR = 8 s and 32 NSA. The average value of the volunteer data for each TR is represented as a horizontal black line. Using the SNR per minute for TR = 8 s as a reference, the expected SNR per scan time for TRs of 2 and 5 s can be calculated given Equation (2). These calculations are shown without T_1w effects ($T_1 << TR$) as a dashed red line, with T_1 = 1.5 s as a densely dotted blue line, and with T_1 = 2.0 s as a sparsely dotted purple line.

4.1 | SNR

In this work, the SNR at each TR was normalized to a TR of 8 s, as > 99% of all metabolite signals are expected to be relaxed after this amount of time. This facilitated direct comparison of the trends in SNR and SNR per minute at different TRs to examine the effects of T_1w more clearly. For a metabolite with a T_1 of 1.5 s, increasing the TR from 2 to 5 s is expected to result in a 22.9% signal increase, while increasing the TR from 5 to 8 s would only result in a 3% increase. The SNR measurements for constant NSA (in Figure 2B) followed these expected trends: A 27% increase in SNR was observed by increasing the TR from 2 to 5 s, and a 2% increase was observed from 5 to 8 s. However, conducting these T_1w calculations under similar acquisition times for a TR of 2 s, the SNR appeared lower than what would be expected for a metabolite with a T_1 of 1.5 s. This nuance was more clearly illustrated when analyzing SNR per unit scan time.

Our results comparing SNR per unit scan time of NAA in spectra acquired with a TR of 2 or 5 s demonstrate that the SNR per minute is only about 17% lower at 5 s than the more common choice of 2 s (SNR/min was 10.8 and 13.0, respectively). The expected SNR per minute with and without T_1w effects shown in Figure 3 demonstrates that the common assumption of a large gain of SNR per minute at TR = 2 s is not realized due to the strong influence of T_1 relaxation. The observed small gain in SNR per minute at TR = 2 s relative to TR = 5 s comes with a steep price of increased T_1w effects, which lead to potential confounders with age, brain region, and disease, as well as a reduced ability to compare across sites. The SNR per minute was lowest at TR = 8 s (SNR/min was 10.1) because at such a long TR, the increase in scan time is larger than any increase in SNR, reducing the SNR per minute.

Despite a relatively large signal from NAA, our SNR per minute data suggest that the T_1 relaxation time is not accurately known. Experiments done in this work and in literature report a T_1 for NAA of 1.39 to 1.53 s; however, the SNR per minute trend with increasing TR is not well fit with a T_1 correction factor of 1.5 s. Using a T_1 value of 2.0 s fits the measured SNR per minute data very well. This discrepancy suggests that measuring metabolite T_1 relaxation times continues to be a challenge. Furthermore, at TR = 5 s, the difference between "no T_1w" and using a T_1 correction value of 2 s is only 8% and is smaller than the spread of the individual data points.

4.2 | Metabolite Estimates

Metabolite estimates for each metabolite are significantly reduced with TR = 2 s, compared to 5 and 8 s. Lower metabolite

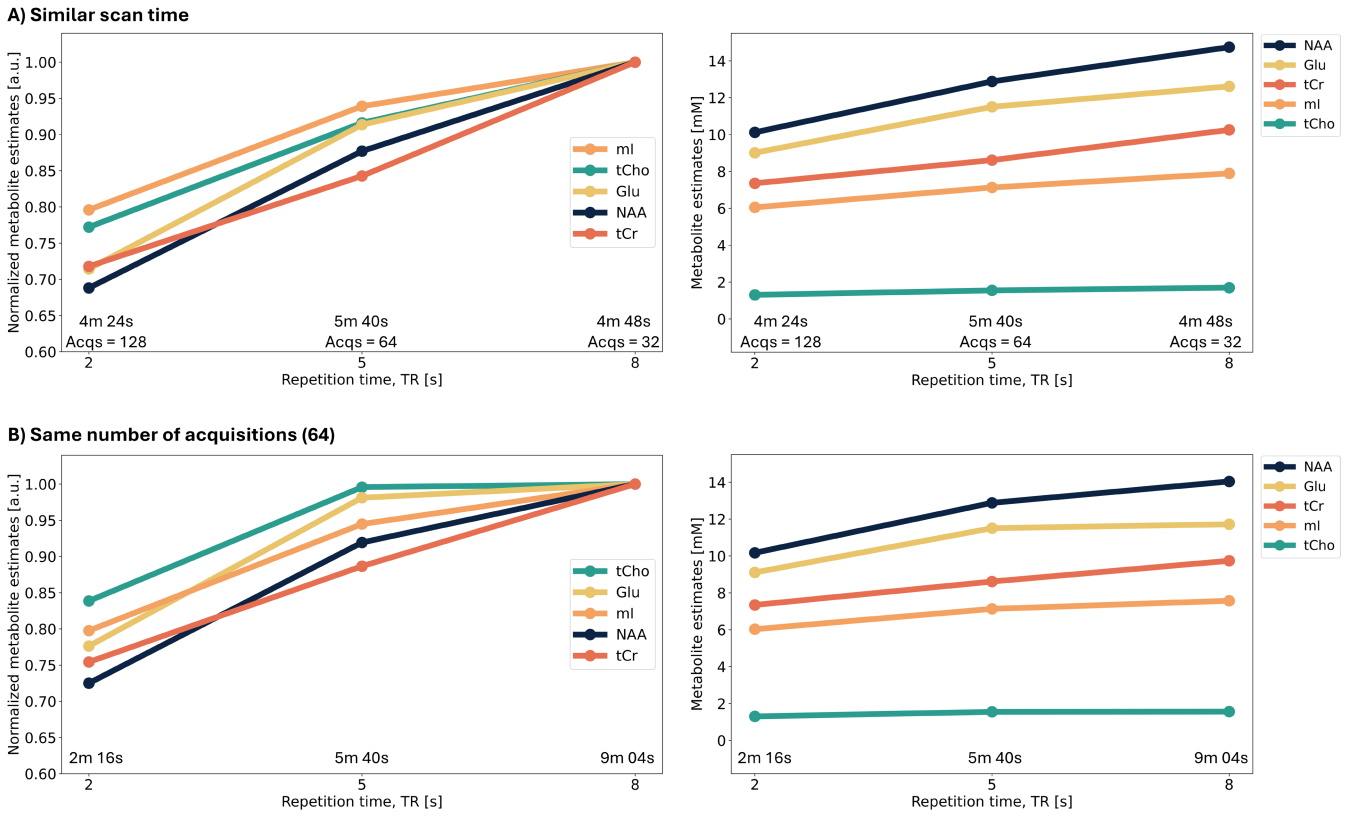

FIGURE 4 | The average reported metabolite estimates as a function of TR for five different metabolites (NAA: N-acetyl aspartate, tCho: total Choline, tCr: total Creatine, mI: myo-inositol, and Glu: glutamate). No metabolite T_1 correction is applied. Similar to how the data is represented in Figure 2, for each metabolite, the FSL-MRS derived metabolite estimates at TR = 2 s and TR = 5 s were normalized to the metabolite estimates found at a TR = 8 s for each volunteer and plotted in the left column. The normalized volunteer data was then averaged together at each TR and plotted. In the right column, reported metabolite estimates are plotted. The data corresponding to a similar scan time with a varying number of acquisitions are shown in panel (A), while the data organized to have 64 acquisitions with different scan times are shown in panel (B).

estimates at TR = 2 s were particularly notable for metabolites with longer T_1s like NAA and tCr. Our results demonstrate that the effect of TR on metabolite estimates was the same, regardless of scan time or number of acquisitions.

It has been accepted in literature that this T_1w-induced reduction in metabolite estimates can be corrected for [1, 23]; however, the most common solution is a single, generic, correction factor that is applied to all metabolites [20, 24–26]. Since each metabolite has a different relaxation time that can change with field strength, brain region, age, pathology, etc., using a single correction factor will result in a spectrum that may or may not yield accurate metabolite estimates for some or all metabolites. Additionally, trying to correct the water reference signal for short repetition times adds more variation to the fit as the T_1 of water, especially in cerebrospinal fluid, is not well characterized [14]. Therefore, any observed difference in metabolite estimate is no longer clearly attributable to changes in tissue biochemistry, as these changes could be a result of improper T_1w correction of that metabolite due to any number of factors that affect T_1 relaxation times. Instead, by increasing the TR, the ambiguity of T_1w correction is removed, as well as the need for correcting metabolite estimates in postprocessing. Thus, the reported metabolite estimate without T_1w correction more accurately reflects the true metabolite estimate for metabolites present in the region of interest. By increasing the accuracy of measured metabolite estimates, a TR of 5 s at 3 T would also improve interstudy agreement and cross-site standardization to increase the impact of MRS studies on our understanding of brain biochemistry.

4.3 | Metabolite T_1

By using metabolite estimates at different TRs, we achieved a reasonable fit to determine the T_1 relaxation times for five metabolites, despite this experiment not being specifically designed to measure T_1 relaxation times. The T_1 relaxation times we determined agree with existing literature values, as shown in Table 2. It is noted that tCr has a short and long T_1-component; however, because this data only has three data points, we were not able to capture these differences. Despite this, the tCr recovery curves fitted relatively well, and the T_1 value agrees with the long-component T_1 value from the Mlynárik study [10] who was able to separate the two components. Our findings demonstrate that it is not necessary to have data points in the short TR regime to obtain a reasonable fit and T_1 result, and that a shorter scan time with fewer time points can be used to determine metabolite T_1s. Despite only including three points in the recovery curve and a longer minimum TR time, the uncertainty obtained here was on the order of 10%–15%, which is in line with or less than previously reported results. This highlights the difficulty in accurately measuring T_1 values in MRS and reinforces the need to move away from correcting for T_1 values. The studies being compared do not mention frequency alignment in their

TABLE 2 | Reported values of T_1s in current study and existing literature in grey matter for both progressive saturation (PS) and inversion recovery (IR) methods. The number of points refers to the number of data points used in the fit; TI is inversion time and is specific to the inversion recovery method. Scan time was calculated as the sum of TR multiplied by the number of acquisitions at each TR, unless otherwise stated in their methods. For the work by Traber et al., they pooled eight regions together for their calculation, so the scan time they reported was multiplied by 8 (NAA: N-acetyl aspartate, tCho: total Choline, tCr: total Creatine, mI: myo-inositol, and Glu: glutamate).

					Literature T_1 relaxation times					
Author	**Region**	**Method, # points**	**TI (s)**	**TR (s)**	**Scan time (min)**	**NAA T_1 (s)**	**tCho T_1 (s)**	**tCr T_1 (s)**	**mI T_1 (s)**	**Glu T_1 (s)**
Current study	Posterior cingulate cortex	PS, 3	—	2, 5, 8	18.13	1.53 ± 0.08	1.16 ± 0.17	1.36 ± 0.12	1.24 ± 0.12	1.38 ± 0.12
Knight-Scott et al. [8]	Posterior cingulate cortex	PS, 5	—	1.5–8	45	1.49 ± 0.14	1.03 ± 0.13	1.39 ± 0.14	1.12 ± 0.22	1.28 ± 0.10
Ethofer et al. [9]	Occipital GM	PS, 6	—	1–10	24	1.47 ± 0.08	1.25 ± 0.22	1.33 ± 0.13	1.12 ± 0.25	—
Mlynárik et al. [10]	Occipital GM	IR, 5	0.15–1.65	6	32	1.47 ± 0.06	1.30 ± 0.06	1.46 ± 0.07	1.19 ± 0.09	1.27 ± 0.10
Träber et al. [11]	Pooled, various	PS, 6	—	0.6–5	45.07	1.39 ± 0.03	1.15 ± 0.04	1.47 ± 0.07	1.36 ± 0.25	—

analyses. As a result, we expect that our approach of exporting every transient to perform frequency alignment during data processing likely improved spectral quality, leading to a more accurate representation of metabolite estimates and thus a more reproducible fit of the T_1 recovery curves. Frequency alignment reduces line broadening due to averaging of misaligned spectra from the effects of participant motion and B_0 drift, which are potentially more prevalent in long TR measurements. However, the uncertainty in the reported T_1 values is still too large to comfortably make definitive claims about T_1 relaxation times of metabolites. This further reinforces the idea that accurately determining the T_1 relaxation times to properly correct for T_1w effects is very challenging.

Analysis of the measured SNR, given Equation (1), in addition to the findings of SNR per unit time in Figure 3, suggests that the NAA SNR data is better modelled with a T_1 closer to 2 s. This disagrees with the result of the T_1 analysis in Table 2 and Figure 5, which reports a T_1 time of NAA closer to 1.5 s. However, this SNR method is not the optimal way to measure T_1. Instead, the discrepancy suggests the need for a more robust measurement of metabolite T_1s.

5 | Limitations

Several potential methodological factors should be considered when interpreting these findings. Only three different TRs were examined, so including additional TRs could provide more detailed insight into the relationship between TR and metabolite estimates, as well as to characterize the trends in SNR per minute. More TRs would also improve the saturation recovery curve fits for determining metabolite T_1 relaxation times.

Time limitations during data acquisition did not allow us to check for subject motion between the start and end of each MRS acquisition, so it is possible that bulk motion limited the achievable SNR for the 9-min TR = 8 s, NSA = 64 acquisition. While we did not use any on-scanner frequency correction, exporting every acquisition allowed for frequency alignment in postprocessing, minimizing the effects of motion.

Additionally, comparing identical scan times across TRs would be preferred, such as 120 NSA for TR = 2 s, 48 NSA for TR = 5 s, and 30 NSA for TR = 8 s, yielding a scan time of ~ 4 min. However, the 32-step phase cycle of the semi-LASER sequence limited our ability to do this. Future studies could investigate the effects of a truncated semi-LASER phase cycle and re-evaluate these results with an identical scan time.

The PCC was chosen to ensure sufficient SNR for all TR and NSA combinations. Future research should investigate the generalizability of these findings across other brain regions. As well, only five metabolites were evaluated in this work, so recommendations cannot be applied to other metabolites and in other brain regions, unless their T_1 values are known with certainty. Our volunteers were of a similar age group and all were healthy, so conclusions can only be made for this specific cohort. Future work should investigate other age groups. Additionally, a larger number of study participants would help reduce uncertainty in averages and fits. Finally, only one previous publication used the

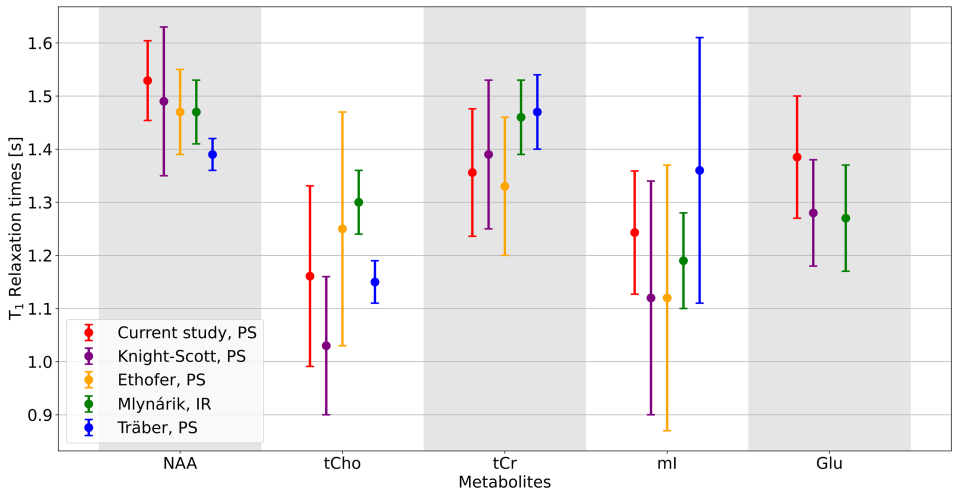

FIGURE 5 | A comparison of T_1 relaxation times between existing literature values and what was found in this work for five metabolites (NAA: N-acetyl aspartate, tCho: total Choline, tCr: total Creatine, mI: myo-inositol, and Glu: glutamate). These results reflect the values that are reported in Table 2. In this work, metabolite estimates for each metabolite were fit to Equation (1), for each volunteer. The resulting relaxation parameter for each volunteer was averaged together and reported with the standard deviation as the error bars.

same brain region as our study, which means comparisons of T_1 values between our study and other literature could be affected by differences in brain regions and T_1 determination strategies.

6 | Conclusion

Results from this study demonstrate that using a TR = 5 s for semi-LASER MRS falls in the Goldilocks zone to balance scan time against T_1 recovery: 5 s allows for sufficient signal recovery to be robust to T_1w effects, and it performed well in terms of SNR, SNR per minute, and metabolite estimates, while still having a clinically feasible scan time of 5 m 40 s. Using TR = 2 s resulted in metabolite estimates and SNR per minute with the largest T_1w effects. TR = 8 s had the least amount of T_1w effects, but experienced diminishing gains leading to reduced SNR per minute. Acquiring semi-LASER MRS with a TR = 5 s is recommended when measuring NAA, tCr, tCho, mI, and Glu due to better SNR per minute and reduced T_1w effects, removing the need for ambiguous, and potentially inaccurate, T_1 correction strategies.

Acknowledgments

The authors thank the study participants for volunteering their time. This work was conducted on the traditional, ancestral, and unceded territories of Coast Salish Peoples, including the territories of the xwməθkwəy̓əm (Musqueam), Skwxwú7mesh (Squamish), Stó:lō and Səl̓ílwətaʔ/Selilwitulh (Tsleil- Waututh) Nations.

Data Availability

Spreadsheets containing all processed and fitted results are available at https://github.com/alexensworth/TRISP, along with the analysis script used to produce the fits with FSL-MRS. Additionally, further analysis of the results is available at https://tr-in-mrs.streamlit.app/ in the form of an interactive application, where all plots included in this manuscript can be recreated, as well as some additional analysis. For example, spectra for all TRs and volunteers, including fits and residuals, can be found on the app. The python code used to create the app is also available at the GitHub link above.

References

1. M. Wilson, O. Andronesi, P. B. Barker, et al., "Methodological Consensus on Clinical Proton MRS of the Brain: Review and Recommendations," *Magnetic Resonance in Medicine* 82, no. 2 (2019): 527–550, https://doi.org/10.1002/mrm.27742.

2. G. Öz, D. K. Deelchand, J. P. Wijnen, et al., "Advanced Single Voxel 1H Magnetic Resonance Spectroscopy Techniques in Humans: Experts' Consensus Recommendations," *NMR in Biomedicine* 34, no. 5 (2021): 1–18, https://doi.org/10.1002/nbm.4236.

3. K. Landheer, M. Gajdošík, and C. Juchem, "A Semi-LASER, Single-Voxel Spectroscopic Sequence With a Minimal Echo Time of 20.1 ms in the Human Brain at 3T," *NMR in Biomedicine* 33, no. 9 (2020): 1–12, https://doi.org/10.1002/nbm.4324.

4. R. M. Camicioli, J. R. Korzan, S. L. Foster, et al., "Posterior Cingulate Metabolic Changes Occur in Parkinson's Disease Patients Without Dementia," *Neuroscience Letters* 354, no. 3 (2004): 177–180, https://doi.org/10.1016/j.neulet.2003.09.076.

5. I. I. Kirov, S. Liu, A. Tal, et al., "Proton MR Spectroscopy of Lesion Evolution in Multiple Sclerosis: Steady-State Metabolism and Its Relationship to Conventional Imaging," *Human Brain Mapping* 38, no. 8 (2017): 4047–4063, https://doi.org/10.1002/hbm.23647.

6. G. H. Hatay and E. Ozturk-Isik, "Optimized Multi-Voxel TE-Averaged PRESS for Glutamate Detection in the Human Brain at 3T," *Journal of Magnetic Resonance* 356 (2023): 107574, https://doi.org/10.1016/j.jmr.2023.107574.

7. R. Fardanesh, M. A. Marino, D. Avendano, D. Leithner, K. Pinker, and S. B. Thakur, "Proton MR Spectroscopy in the Breast: Technical Innovations and Clinical Applications," *Journal of Magnetic Resonance Imaging* 50, no. 4 (2019): 1033–1046, https://doi.org/10.1002/jmri.26700.

8. J. Knight-Scott, P. Brennan, S. Palasis, and X. Zhong, "Effect of Repetition Time on Metabolite Quantification in the Human Brain in 1H MR Spectroscopy at 3 Tesla," *Journal of Magnetic Resonance Imaging* 45, no. 3 (2017): 710–721, https://doi.org/10.1002/jmri.25403.

9. T. Ethofer, I. Mader, U. Seeger, et al., "Comparison of Longitudinal Metabolite Relaxation Times in Different Regions of the Human Brain

at 1.5 and 3 Tesla," *Magnetic Resonance in Medicine* 50, no. 6 (2003): 1296–1301, https://doi.org/10.1002/mrm.10640.

10. V. Mlynárik, S. Gruber, and E. Moser, "Proton T1 and T2 Relaxation Times of Human Brain Metabolites at 3 Tesla," *NMR in Biomedicine* 14, no. 5 (2001): 325–331, https://doi.org/10.1002/nbm.713.

11. F. Träber, W. Block, R. Lamerichs, J. Gieseke, and H. H. Schild, "1H Metabolite Relaxation Times at 3.0 Tesla: Measurements of T1 and T2 Values in Normal Brain and Determination of Regional Differences in Transverse Relaxation," *Journal of Magnetic Resonance Imaging* 19, no. 5 (2004): 537–545, https://doi.org/10.1002/jmri.20053.

12. Y. Li, E. Ozturk-Isik, J. M. Lupo, A. P. Chen, D. B. Vigneron, and S. J. Nelson, "T1 and T2 Metabolite Relaxation Times in Normal Brain at 3T and 7T," *Journal of Molecular Imaging and Dynamics* 02, no. 02 (2013): 1–5, https://doi.org/10.4172/2155-9937.S1-002.

13. L. An, M. F. Araneta, M. Victorino, and J. Shen, "Determination of Brain Metabolite T1 Without Interference From Macromolecule Relaxation," *Journal of Magnetic Resonance Imaging* 52, no. 5 (2020): 1352–1359, https://doi.org/10.1002/jmri.27259.

14. J. Near, A. D. Harris, C. Juchem, et al., "Preprocessing, Analysis and Quantification in Single-Voxel Magnetic Resonance Spectroscopy: Experts' Consensus Recommendations," *NMR in Biomedicine* 34, no. 5 (2021): 1–23, https://doi.org/10.1002/nbm.4257.

15. L. Sporn, E. L. MacMillan, R. Ge, K. Greenway, F. Vila-Rodriguez, and C. Laule, "Longer Repetition Time Proton MR Spectroscopy Shows Increasing Hippocampal and Parahippocampal Metabolite Concentrations With Aging," *Journal of Neuroimaging* 29, no. 5 (2019): 592–597, https://doi.org/10.1111/jon.12648.

16. E. E. Brief, K. P. Whittall, D. K. B. Li, and A. MacKay, "Proton T1 Relaxation Times of Cerebral Metabolites Differ Within and Between Regions of Normal Human Brain," *NMR in Biomedicine* 16, no. 8 (2003): 503–509, https://doi.org/10.1002/nbm.857.

17. D. K. Deelchand, A. Berrington, R. Noeske, et al., "Across-Vendor Standardization of Semi-LASER for Single-Voxel MRS at 3T," *NMR in Biomedicine* 34, no. 5 (2021): 1–11, https://doi.org/10.1002/nbm.4218.

18. Y. Zhang, M. Brady, and S. Smith, "Segmentation of Brain MR Images Through a Hidden Markov Random Field Model and the Expectation-Maximization Algorithm," *IEEE Transactions on Medical Imaging* 20, no. 1 (2001): 45–57, https://doi.org/10.1109/42.906424.

19. R. Simpson, G. A. Devenyi, P. Jezzard, T. J. Hennessy, and J. Near, "Advanced Processing and Simulation of MRS Data Using the FID Appliance (FID-A)—An Open Source, MATLAB-Based Toolkit," *Magnetic Resonance in Medicine* 77, no. 1 (2017): 23–33, https://doi.org/10.1002/mrm.26091.

20. W. T. Clarke, C. J. Stagg, and S. Jbabdi, "FSL-MRS: An End-to-End Spectroscopy Analysis Package," *Magnetic Resonance in Medicine* 85, no. 6 (2021): 2950–2964, https://doi.org/10.1002/mrm.28630.

21. W. W. F. Pijnappel, A. van den Boogaart, R. de Beer, and D. van Ormondt, "SVD-Based Quantification of Magnetic Resonance Signals," *Journal of Magnetic Resonance (1969).* 97, no. 1 (1992): 122–134, https://doi.org/10.1016/0022-2364(92)90241-X.

22. R. R. Ernst, G. Bodenhausen, and A. Wokaun, *Principles of Nuclear Magnetic Resonance in One or Two Dimensions* (Clarendon, 1991).

23. A. D. Harris and E. L. MacMillan, "Chapter 4—MRS in Neuroinflammation," in *Advances in Magnetic Resonance Technology and Applications*, vol. 9, eds. C. Laule and J. D. Port (Academic Press, 2023): 79–116, https://doi.org/10.1016/B978-0-323-91771-1.00012-5.

24. S. W. Provencher, "Estimation of Metabolite Concentrations From Localized In Vivo Proton NMR Spectra," *Magnetic Resonance in Medicine* 30, no. 6 (1993): 672–679, https://doi.org/10.1002/mrm.1910300604.

25. M. Wilson, G. Reynolds, R. A. Kauppinen, T. N. Arvanitis, and A. C. Peet, "A Constrained Least-Squares Approach to the Automated Quantitation of In Vivo 1H Magnetic Resonance Spectroscopy Data," *Magnetic Resonance in Medicine* 65, no. 1 (2011): 1–12, https://doi.org/10.1002/mrm.22579.

26. B. J. Soher, P. Semanchuk, D. Todd, et al., "Vespa: Integrated Applications for RF Pulse Design, Spectral Simulation and MRS Data Analysis," *Magnetic Resonance in Medicine* 90, no. 3 (2023): 823–838, https://doi.org/10.1002/mrm.29686.